ADVANCED FUNCTIONAL MATERIALS
www.afm-journal.de

Doping-Free Organic Light-Emitting Diodes with Very High Power Efficiency, Simple Device Structure, and Superior Spectral Performance

Qi Wang, Iain W. H. Oswald, Michael R. Perez, Huiping Jia, Ahmed A. Shahub, Qiquan Qiao, Bruce E. Gnade, and Mohammad A. Omary**

Today's state-of-the-art phosphorescent organic light-emitting diodes (PhOLEDs) must rely on the host-guest doping technique to decrease triplet quenching and increase device efficiency. However, doping is a sophisticated device fabrication process. Here, a Pt(II)-based complex with a near unity photoluminescence quantum yield and excellent electron transporting properties in the form of neat film is reported. Simplified doping-free white PhOLED and yellow-orange PhOLED based on this emitter achieve rather low operating voltages (2.2–2.4 V) and very high power efficiencies of approximately 80 lm W^{-1} (yellow-orange) and 50 lm W^{-1} (white), respectively, without any light extraction enhancement. Furthermore, the efficient white device also exhibits high color stability. No color shift is observed during the entire operation of the device. Analysis of the device's operational mechanism has been postulated in terms of exciton and polaron formation and fate. It is found that using the efficient neat Pt(II)-complex as a homogeneous emitting and electron transporting layer and an ambipolar blue emitter are determining factors for achieving such a high efficiency.

1. Introduction

Phosphorescent organic light-emitting diodes (PhOLEDs) are able to achieve high efficiency by converting 100% of the injected electrons into photons via relaxation of both singlet and triplet excitons, holding great potential for lighting and display applications.[1] However, because the spin-forbidden phosphorescence is a much slower decay process (≈μs) than the spin-conserving fluorescence (≈ns), common phosphorescent dyes must be doped into host material(s) to enhance the luminance efficiency by decreasing severe triplet quenching induced by strong exciton-aggregation.[2] To date, nearly all state-of-the-art PhOLEDs rely on such a design strategy.[3] Among problems with doping methods is the difficulty of precise control of the relative guest/host doping concentration. This problem becomes even more complicated in a white device as doping in each emissive layer (EML) needs to be optimized separately for balanced white emission and improved device efficiency.[1d] These issues present significant barriers to large-scale commercialization of PhOLEDs, making undoped device structures highly promising.[4–6] Pioneering work in 2001 by Y. Wang and co-workers reported a green neat PhOLED with a 4 lm W^{-1} power efficiency (PE).[5a] Yellow and red undoped PhOLEDs were subsequently reported with external quantum efficiencies (EQEs) of 1.6% (yellow), 6.3% (red) and PEs of 3.5 lm W^{-1} (yellow), 2.7 lm W^{-1} (red).[5b,c] Recently, based on efficient excimer emissions from Pt(II) organometallic emitters, Cocchi and co-workers demonstrated a neat PhOLED with EQE and PE of 16.0% and 8.1 lm W^{-1}, respectively,[5d] whereas Yang et al. reported an undoped red OLED with 17.5% and 45 lm W^{-1} maximum EQE and PE, respectively.[6a] For undoped white PhOLEDs, the reported highest efficiency is 14% for EQE and 25 lm W^{-1} for PE.[6a]

As shown in **Table 1**, although both the EQE and PE of undoped PhOLEDs have experienced substantial improvements during the past decade, they remain far below those of their doped counterparts; in particular for PE.[7,8] This is primarily due to the difficulty in finding a phosphorescent emitter that simultaneously possesses charge-transporting ability and high photoluminescence (PL) efficiency as reflected in PL quantum yield (η_{QY}) in the neat form.[1d,5a,9] For example, in the neat device found elsewhere,[6a] the optimized thickness of the EML was only 1.5 nm due to the restriction of the charge-transporting ability of the neat emitter used. However, Yang found

Dr. Q. Wang, I. W. H. Oswald, A. A. Shahub, Prof. M. A. Omary
Department of Chemistry
University of North Texas
Denton, TX 76203, USA
E-mail: Omary@unt.edu
Dr. Q. Wang, Prof. Q. Q. Qiao
Department of Electrical Engineering and Computer Sciences
College of Engineering
South Dakota State University
Brookings, SD 57007, USA
Dr. M. R. Perez, Dr. H. P. Jia, Prof. B. E. Gnade
Department of Materials Science and Engineering and Erik Jonsson School of Engineering and Computer Science
University of Texas at Dallas,
Richardson, TX 75083, USA
E-mail: Gnade@utdallas.edu

DOI: 10.1002/adfm.201400597

Table 1. Most advanced, selected performance characteristics of phosphorescent OLEDs.

Reported Device	Color	V_t [V][a)]	PE [lm W^{-1}] (at peak, 500 cd m^{-2}, 1000 cd m^{-2})[b)]	CIE (x,y)[c)]	Color shift (x,y)[d)]
Ref. [7c] (doped)	Orange	3.0	61.7 – -	(0.50,0.50)	–
Ref. [7d] (doped)	Orange	3.8	43.6 – 15.0	(0.60,0.39)	–
Ref. [7e] (doped)	Orange	2.5	47.2 – -	(0.49,0.48)	–
Ref. [6a] (undoped)	Orange	–	45.0 – 18.7	(0.46,0.47)	–
This work	Orange	**2.2**	**79.2 ± 0.2, 57.6 ± 0.3, 50.1 ± 0.3**	(0.49,0.50)	–
Ref. [8c] (doped)	White	2.4	67.2, 40.1, 33.5	(0.47,0.44)	> (0.06,0.01)
Ref. [8d] (doped)	White	2.8	59.9, 48.0, 43.3	(0.40,0.40)	> (0.03,0.03)
Ref. [8e] (doped)	White	3.5	43.0 – 23.2	(0.38,0.44)	–
Ref. [6a] (undoped)	White	–	25.0 – -	(0.42,0.41)	> (0.02,0.01)
This work (DFW-1)	**White**	**2.4**	**49.5 ± 0.1, 34.0 ± 0.2, 30.0 ± 0.3**	**(0.44,0.47)**	**(0.00,0.00)**

[a)] V_t: turn-on voltage at 1 cd m^{-2}; [b)] PE: power efficiency; [c)] CIE: Commission Internationale de L'Eclairage; [d)] Color shift: reflected by the shift of the CIE coordinates in the range of 1–10 000 cd m^{-2}.

that this ultrathin EML allowed charge and exciton leakage outside the emissive region, leading to a decrease in efficiency at high current densities.[6a] Although Liu et al. designed a double-quantum-well structure to improve charge and exciton confinement within the neat EMLs,[6b] the device efficiency was still relatively low (PE = 30.5 lm W^{-1}) due to the poor carrier mobility and the strong triplet quenching of the neat emitter used.[2,5a,9] To overcome these problems, here we describe the use of a neat metal-organic Pt(II)-pyridylazolate phosphor possessing a nearly unity η_{QY} and excellent electron-transporting ability. A simplified doping-free white OLED (DFW-OLED) and yellow-orange PhOLED based on this emitter realize rather low operating voltages (2.2–2.4 V) and very high power efficiencies of approximately 80 lm W^{-1} (yellow-orange) and 50 lm W^{-1} (white), respectively, without any out-coupling enhancement. Analysis of the device working mechanism is then performed in both devices, from which the determining factors leading to such high efficiencies are described.

2. Results and Discussion

2.1. Photoluminescence Efficiency of the Pt(II)-Phosphor in the Neat Thin Film

The key phosphor used is bis[3,5-bis(2-pyridyl)-1,2,4-triazolato] platinum(II), [Pt(ptp)$_2$] (see **Figure 1** inset). Under 341 nm optical excitation, a neat Pt(ptp)$_2$ film (100 nm) exhibits a PL maximum at 593 nm with a η_{QY} of 98 ± 2% (see Experimental Section and Supporting Information Figure S1). This is in sharp contrast with common phosphors that show low η_{QY} in neat-film forms, for example, Btp$_2$Ir(acac) (red) ~zero, Ir(ppy)$_3$

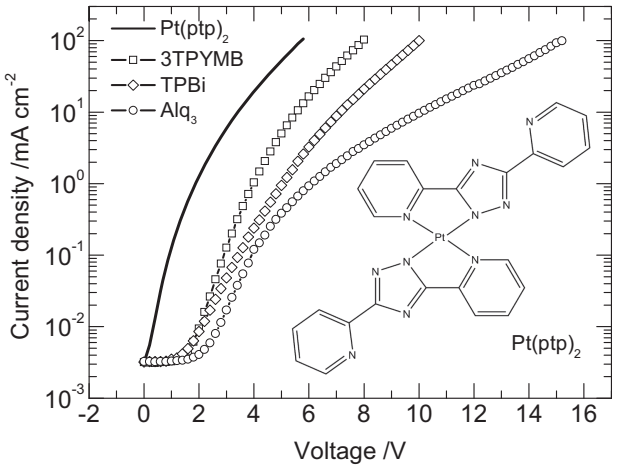

Figure 1. Current density–voltage characteristics of four electron-only devices based on Pt(ptp)$_2$, 3TPYMB, TPBi and Alq$_3$, respectively. The single-carrier device structure used is Al/LiF/*X* (100 nm)/LiF/Al. Inset: molecular structure of Pt(ptp)$_2$.

(green) < 3%, FIrpic (blue) ≈16% (see Experimental Section for materials composition).[9c,d] Generally, η_{QY} can be defined in terms of the rate constants of the phosphorescence radiative (k_R) and the sum of the non-radiative ($\sum_{NR}^{k}$) processes, $\eta_{QY} = k_R / (k_R + \sum_{NR}^{k})$. In neat phosphorescent systems, non-radiative processes in PL are mainly ascribed to triplet–triplet (*T*–*T*) quenching. The almost unity η_{QY} indicates $\sum_{NR}^{k} \ll k_R$ and that *T*–*T* quenching is insignificant in neat Pt(ptp)$_2$. This result significantly differs from that in, for example, neat Ir(ppy)$_3$ system reported previously.[9c,d] Compared to neat Ir(ppy)$_3$, the high η_{QY} of neat Pt(ptp)$_2$ can be explained as follows.

First, the emission mechanisms in neat Ir(ppy)$_3$ and Pt(ptp)$_2$ are different. In neat Ir(ppy)$_3$ monomers still dominate the emission,[9d] hence concentration-induced *T*-*T* quenching is expected with increasing triplet density, rendering $\sum_{NR}^{k} \gg k_R$ as observed previously.[9c] In contrast, Pt(ptp)$_2$ molecules in the neat form are symmetrically stacked with strong $\cdots$Pt(II)$\cdots$Pt(II)$\cdots$Pt(II)$\cdots$ intermolecular interactions such that the neat material's emission originates from a Pt–Pt bonded species.[5b,10] Second, *T*-*T* quenching is also influenced by molecular separation. However, it is calculated that the average spacing (D_s) between phosphorescent molecules in neat Pt(ptp)$_2$ and Ir(ppy)$_3$ is comparable (≈1 nm) according to $D_s = (\rho N_A / M_m)^{-1/3}$,[2a,9d] where ρ is the mass density ($\rho \approx 1.0$ g cm^{-3}), M_m the molar mass, and N_A the Avogadro's number. Furthermore, the much shorter decay lifetime of neat Pt(ptp)$_2$ versus [Ir(ppy)$_3$] (469 ns versus 1500 ns) is another factor for the reduction of *T*–*T* quenching by reducing the probability of triplet-triplet interactions.[2b,9d] Finally, *T*-*T* annihilation generally occurs via $^3M^* + {}^3M^* \rightarrow M^* + M$,[2,9d] where $^3M^*$ represents the triplet excited state, *M* the ground state of the molecule, and k_{TTA} the quenching rate constant. Therefore, *T*–*T* annihilation strength can be reflected by k_{TTA}.[2a] k_{TTA}s in neat Pt(ptp)$_2$ and Ir(ppy)$_3$ have been determined to be ≈10^{-12} cm^3 s^{-1} by our group and ≈10^{-10} cm^3 s^{-1} by Holzer et al., respectively.[9d,11] However, the initial exciton densities are different in both cases, for example, 10^{17} cm^{-3} (Pt(ptp)$_2$) versus 10^{19} (Ir(ppy)$_3$) cm^{-3}, which makes the direct comparison of k_{TTA}s difficult. Despite lack of this information, the low k_{TTA} of neat Pt(ptp)$_2$ could be one factor for achieving the high η_{QY}.[2,9c]

2.2. Charge-Transporting Property of the Pt(II)-Phosphor

Besides possessing a high η_{QY}, $Pt(ptp)_2$ is also an excellent electron-transporting material, as substantiated by the following. First, under the same driven voltage the electron current in an electron-only device is orders of magnitude higher than the hole current in a hole-only device (which in fact shows negligible current across a wide range of voltages) based on neat $Pt(ptp)_2$ with the same thickness; see details in Supporting Information Figure S2. Second, it was reported that the electron mobility of neat $Pt(ptp)_2$ is in the order of 10^{-5}–10^{-4} cm^2 V^{-1} s^{-1}.[11] This value is slightly higher than that of 3TPYMB, TPBi and Alq_3 which can serve as efficient electron-transporting layers (ETLs) as established previously.[12] Moreover, we find that neat $Pt(ptp)_2$ can form a Ohmic contact with LiF/Al. To illustrate this point, electron-only devices based on $Pt(ptp)_2$, 3TPYMB, TPBi and Alq_3 using the same structure of Al/LiF/*X* (100 nm)/LiF/Al were fabricated. Figure 1 shows the current density-voltage characteristics of the devices. Considering the different band gaps and energy levels of these materials, in the $Pt(ptp)_2$ device the initial increase of electron current at the onset of the applied voltage indicates an Ohmic contact between $Pt(ptp)_2$ and LiF/Al.[2b] Furthermore, the current density of the $Pt(ptp)_2$ device is orders of magnitude higher than that of the other devices during the entire process. These results show that $Pt(ptp)_2$ possesses high electrical conductivity and can serve as an efficient ETL when combining with LiF/Al.

2.3. Device Design and Characterization of Doping-Free Orange and White OLEDs

As can be seen, the neat $Pt(ptp)_2$ film exhibits an almost unity PL efficienty and superior electron transporting property. Consequently, an undoped monochromatic PhOLED based on $Pt(ptp)_2$ was designed as follows: ITO/TAPC/mCP/$Pt(ptp)_2$/LiF/Al, with the neat $Pt(ptp)_2$ serving as both the EML and ETL. The optimized device shows an electroluminescence peak of 580 nm with a forward viewing EQE of 20.5 ± 0.1%, and PE of 79.2 ± 0.2 lm W^{-1} (**Figure 2**). At a brightness of 1000 cd m^{-2}, the device PE still reaches as high as 50.1 ± 0.3 lm W^{-1}. As shown in Table 1, compared to the most advanced PhOLEDs reported to date with similar yellow/orange/red wavelength, the doping-free $Pt(ptp)_2$ device exhibits the lowest turn-on voltage, highest efficiency, and lowest efficiency roll-off.

White devices based on $Pt(ptp)_2$ can be realized by incorporating a neat blue EML such as FIrpic or FIr6. The first white stack as such, DFW-OLED1, has a device structure of ITO/TAPC/mCP/FIrpic/$Pt(ptp)_2$/LiF/Al (Figure 2). DFW-OLED1 exhibits a yellowish warm-white emission with unchanged EL spectra at all voltages studied (Figure 2c). It is noteworthy that this high color stability was rarely seen for high-efficiency white PhOLEDs.[1d,8] This indicates that the exciton recombination zone(s) in DFW-OLED1 is/are not influenced by changing voltages (vide infra). Besides the superior spectral performance, the peak forward viewing PE of DFW-OLED1 is 49.5 ± 0.1 lm W^{-1} (Figure 2a), which is twice that of the highest efficiency of the reported undoped white OLED (25 lm W^{-1}).[6a] Furthermore, at a practically useful luminance of 1000 cd m^{-2}, the device

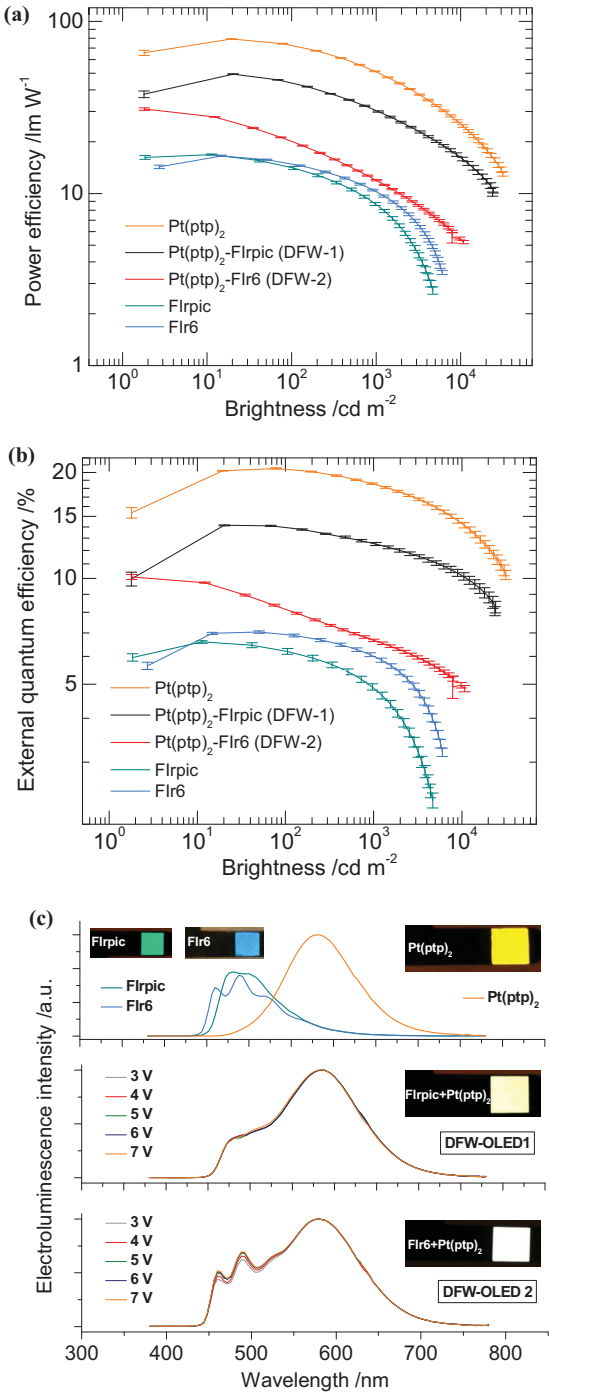

Figure 2. Power efficiencies a), and external quantum efficiencies b) versus brightness of the optimized neat $Pt(ptp)_2$ device (ITO/TAPC (40 nm)/mCP (10 nm)/$Pt(ptp)_2$ (100 nm)/LiF/Al), DFW-OLED1 (ITO/TAPC (40 nm)/mCP (10 nm)/FIrpic (8 nm)/$Pt(ptp)_2$ (90 nm)/LiF/Al), DFW-OLED2 (ITO/TAPC (40 nm)/mCP (10 nm)/FIr6 (8 nm)/$Pt(ptp)_2$ (90 nm)/LiF/Al), neat FIrpic device (ITO/TAPC (40 nm)/mCP (10 nm)/FIrpic (8 nm)/3TPYMB (40 nm)/LiF/Al), and neat FIr6 device (ITO/TAPC (40 nm)/mCP (10 nm)/FIr6 (8 nm)/3TPYMB (40 nm)/LiF/Al). c) Spectral performances of these devices. Inset: image of each device with 10 mm^2 active area. The Commission Internationale de L'Eclairage coordinates (CIE) and Color-Rendering Index (CRI) of DFW-OLED1 and 2 are (0.44, 0.45), 65 and (0.40, 0.44), 73, respectively. See Supporting Information Figure S3 and S6 for the design principle of both the FIrpic and FIr6 devices.[12]

PE can still reach 30.0 ± 0.3 lm W^{-1}. Compared with today's state-of-the-art doped white OLEDs (Table 1), the DFW-OLED1 herein reveals a superior trade-off among simplicity/efficiency/color-stability factors that are critical for commercialization.

Realizing such high PEs in both devices can be explained by the following. First, eliminating host materials that possess high energy gaps allows a direct charge recombination on the molecular sites of phosphorescent dyes. This process reduces the host-guest exchange energy loss in PE.[13] Second, the high quantum yield of neat $Pt(ptp)_2$ assures that the electrically generated excitons can be utilized efficiently by radiative decay. Furthermore, the rather low turn-on voltages of both devices are also key because a low operating voltage is a prerequisite to achieving a high PE.[1d,9a] For the pure $Pt(ptp)_2$ and white devices, the turn-on voltages at 1 cd m^{-2} are 2.2 and 2.4 V, respectively, which are the lowest compared to literature values.[8c] We note that using a single $Pt(ptp)_2$ layer as a homogeneous EML/ETL is one determining factor for voltage reduction because 1) $Pt(ptp)_2$ is a superior electron transporting material and it can form Ohmic contact with LiF/Al cathode (Figure 1); 2) the homogeneous EML/ETL design can eliminate interfacial energy barriers associated with heterojunctions and suppress interfacial charge accumulation due to the mismatched energy levels, thus greatly smoothing charge transport.[14] To verify this point, the single $Pt(ptp)_2$ layer in DFW-OLED1 is replaced with a $Pt(ptp)_2$/ETL (ETL: Alq_3, TPBi or 3TPYMB) bilayer combination without altering the other layers. **Figure 3** shows the efficiency (Figure 3a) and electroluminescence spectra (Figure 3b) of the three control devices. The turn-on voltages of the resulting control devices all exceed 3 V, and the peak PEs dramatically decrease to 23–28 lm W^{-1}. Both results confirm that a homogeneous EML/ETL is essential for achieving the high efficiency of the device. Moreover, in all of these control devices, color shifts are clearly observed with increasing voltage. This indicates that a homogeneous EML/ETL is also crucial for the color stability in such white devices by eliminating interfacial energy barriers.[12b,c]

Based on the architecture of DFW-OLED1, FIrpic was replaced with a deeper-blue emitter FIr6 to construct DFW-OLED2 (ITO/TAPC/mCP/FIr6/$Pt(ptp)_2$/LiF/Al) since FIr6 can better complement the yellow-orange emission of $Pt(ptp)_2$ (Figure 2c).[15] However, the efficiency of DFW-OLED2 is significantly lower than that of DFW-OLED1, that is, 31.0 ± 0.5 lm W^{-1} versus 49.5 ± 0.1 lm W^{-1} (Figure 2a). This is unexpected because the thickness of each layer is the same in DFW-OLED1 and DFW-OLED2, and the efficiencies of the pure FIr6 and FIrpic devices (with the structure of ITO/TAPC/mCP/FIrpic or FIr6/3TPYMB/LiF/Al) are comparable (Figure 2a,b). The lower efficiency of DFW-OLED2 may be attributed to the stronger contribution of the FIr6 emission in DFW-OLED2 than that of FIrpic in DFW-OLED1 (Figure 2c). To test this hypothesis, we fabricated another control device based on DFW-OLED2 by reducing the FIr6 thickness from 8 nm to 6 nm (Supporting Information Figure S4). Although the intensity of the FIr6 emission is decreased, as expected, the efficiency of the resulting device (31.4 ± 0.5 lm W^{-1}) is still comparable to that of DFW-OLED2, ruling out this mechanism.

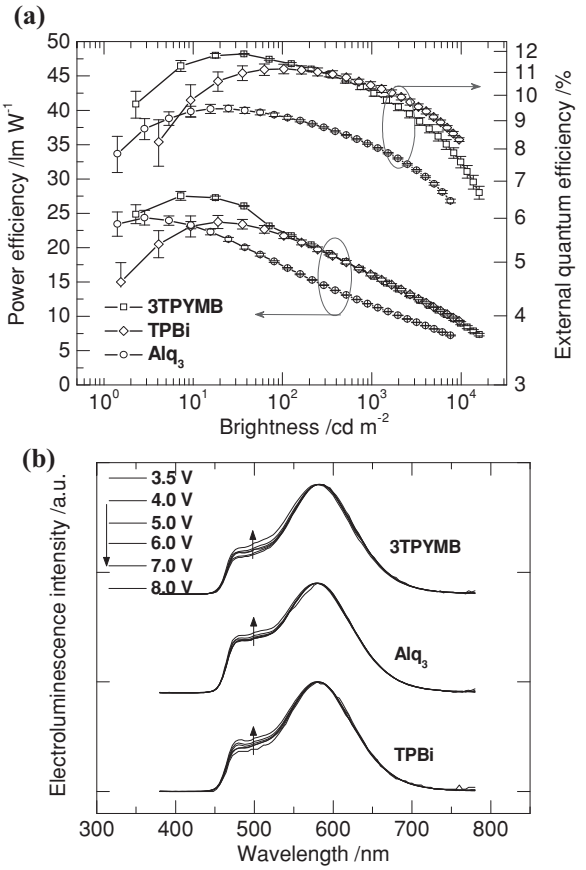

Figure 3. a) Power efficiencies and external quantum efficiencies versus current density of three white control devices with different electron-transporting layers 3TPYMB, TPBi and Alq_3. b) Voltage-dependent spectral performance of each device. To make the relative intensity of the blue emission similar to that of DFW-OLED1 in the spectra, the optimized structure of each control device is ITO/TAPC (40 nm)/mCP (10 nm)/FIrpic (8 nm)/$Pt(ptp)_2$ (30 nm)/3TPYMB (30 nm)/LiF/Al, ITO/TAPC (40 nm)/mCP (10 nm)/FIrpic (8 nm)/$Pt(ptp)_2$ (30 nm)/TPBi (30 nm)/LiF/Al, and ITO/TAPC (40 nm)/mCP (10 nm)/FIrpic (8 nm)/$Pt(ptp)_2$ (40 nm)/Alq_3 (20 nm)/LiF/Al.

2.4. Working Principle of the Doping-Free White OLED

To shed light on this issue, we calculated that the fraction of excitons directly formed on $Pt(ptp)_2$ in DFW-OLED1 is, $\chi_{Pt(ptp)_2-trap,DFW-OLED1} = 54\%$ (see Experimental Section).[8b,13] That is, 54% of the excitons are formed by direct trapping on $Pt(ptp)_2$ molecules, whereas the remaining 46% are formed on FIrpic molecules. The excited FIrpic molecules could either release energy by emission ($\chi_{FIrpic-emission}$) or transfer energy to $Pt(ptp)_2$ ($\chi_{FIrpic-energytransfer}$). However, $\chi_{FIrpic-emission}$ is further calculated to be 46% which indicates that $\chi_{FIrpic-energytransfer}$ is almost negligible. This result shows that $Pt(ptp)_2$ emission in DFW-OLED1 is mainly through direct exciton formation on $Pt(ptp)_2$ molecules and is independent of FIrpic. In DFW-OLED2, however, excitons directly formed on $Pt(ptp)_2$ ($\chi_{Pt(ptp)_2-trap,DFW-OLED2}$) accounts for only 18%. For the remaining 82% excitons formed on FIr6, we further calculated that the fraction of excitons consumed by FIr6 emission and energy-transfer to $Pt(ptp)_2$ is $\chi_{FIr6-emission} = 49\%$ and $\chi_{FIr6-energytransfer} = 33\%$, respectively. This

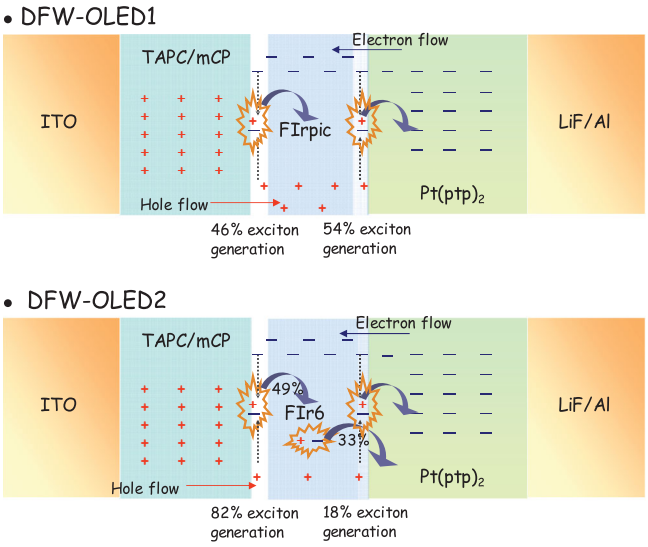

Figure 4. Proposed operational principles of DFW-OLED1 and DFW-OLED2. In DFW-OLED1 FIrpic is an ambipolar material. Therefore, excitons can be generated on both edges of the FIrpic layer (46% vs 54%), then harvested by FIrpic and $Pt(ptp)_2$ molecules, respectively, in an independent manner. In DFW-OLED2 only 18% excitons are generated on the $Pt(ptp)_2$ molecules at the FIr6/$Pt(ptp)_2$ interface. The remaining 82% are directly generated on the FIr6 molecules. Among them, approximately 33% excitons are then energy transferred to $Pt(ptp)_2$, leaving the remaining 49% excitons for FIr6 emission.

calculation result illustrates two points: 1) in DFW-OLED2 the main exciton formation zone is at the mCP/FIr6 interface; 2) the $Pt(ptp)_2$ emission strongly depends on the FIr6-$Pt(ptp)_2$ energy transfer process. **Figure 4** depicts the operational principles of DFW-OLED1 and 2 according to the above analysis.

As can be seen, in DFW-OLED1 the emissions of $Pt(ptp)_2$ and FIrpic are two independent processes and the fractions of excitons directly formed on and consumed by FIrpic and $Pt(ptp)_2$ are nearly equal (Figure 4 DFW-1). However, in DFW-OLED2 the device efficiency is determined by FIr6, which is less efficient than $Pt(ptp)_2$ (Figure 2), because 82% of the overall excitons are directly formed on the FIr6 molecules (Figure 4 DFW-2). Furthermore, the process of FIr6-$Pt(ptp)_2$ energy transfer in DFW-OLED2 can further induce a decrease in PE due to the exchange energy loss.[13] The combination of the aforementioned factors explains the lower efficiency of DFW-OLED2 versus DFW-OLED1. The difference in working mechanisms between both devices is mainly due to the different charge-transporting property of FIrpic and FIr6. FIrpic shows ambipolar characteristics,[8b,16] whereas FIr6 is an electron-dominated material.[15] Hence, in DFW-OLED1 excitons can be generated on both edges of the FIrpic layer while in DFW-OLED2 the main recombination zone is located at the mCP/FIr6 interface. From this, we conclude that the ambipolar blue layer is another determining factor for realizing high efficiency in this type of white device.

We should note that the efficiency of DFW-OLED1 still has room to improve because neat FIrpic is still inefficient due to its intrinsically low η_{QY} (≈16%).[9c] If using an 'ideal' blue emitter with a unity η_{QY} and similar spectrum as FIrpic, approximately 63 lm W^{-1} forward viewing PE can in principle be achieved.[13]

One challenge in our non-doped devices is the efficiency roll-off at high brightness (Table 1). We have demonstrated that triplet-triplet and triplet-polaron (charged $Pt(ptp)_2$ molecules) quenching can account for the efficiency roll-off in the pure $Pt(ptp)_2$ device at high current density.[11] Here, the origin of efficiency roll-off in DFW-OLED1 is complicated. According to the device working mechanism, both the aforementioned quenching processes should still exist in either the FIrpic or $Pt(ptp)_2$ layer due to the independent emission process of both emitters (Figure 4). Moreover, although loss of charge balance can also decrease the device efficiency at high current density,[2c] this factor should be ruled out in DFW-OLED1 because of the ambipolar characteristics of FIrpic.[8b]

3. Conclusion

In summary, a Pt(II)-based phosphor [$Pt(ptp)_2$] is reported which possesses a unity PL quantum efficiency and excellent electron-transporting property in the neat thin film form. Undoped yellow-orange and white PhOLEDs based on $Pt(ptp)_2$ realize very high power efficiencies of 79.2 ± 0.2 lm W^{-1} and 49.5 ± 0.1 lm W^{-1}, respectively, which even outperform (yellow/orange/red) or compete with (white) today's state-of-the-art doped devices. The working mechanisms of both devices are studied. It is found that using the efficient neat Pt(II)-complex as a homogeneous emitting and electron transporting layer and an ambipolar blue emitter are determining factors for realizing such high efficiency. This study demonstrates the possibility of achieving very high-efficiency OLEDs without relying on sophisticated doping techniques, and can be a starting point for achieving simplified, low-cost OLEDs with unprecedented performance.

4. Experimental Section

The main materials used have acronyms as follows: $Btp_2Ir(acac)$: bis[2-(2′-benzothienyl)pyridinato-N,$C^{3'}$](acetylacetonato)iridium(III). $Ir(ppy)_3$: *fac*-tris(2-phenylpyridine)iridium(III). FIrpic: bis[(4,6-difluorophenyl)pyridinato-N,C^2](picolinate)iridium(III). FIr6: bis(2,4-difluorophenylpyridinato)tetrakis(1-pyrazolyl)borate iridium(III). TAPC: 1, 1-bis[(di-4-tolylamino)phenyl]cyclohexane. mCP: 1,3-bis(9-carbazolyl)benzene. 3TPYMB: tris[3-(3-pyridyl)mesityl]borane. TPBi: 2,2′,2″-(1,3,5-Benzinetriyl)-tris(1-phenyl-1-H-benzimidazole). Alq_3: tris(8-hydroxy-quinolinato)aluminium.

Photoluminescence Characterization: Steady-state photoluminescence spectra were acquired with a PTI Quanta-Master model QM-4 scanning spectrofluorometer. The quantum yield measurement followed the method proposed by Kawamura et al.[9b] Before this test, we examined the quantum yield of a 100 nm tris (8-hydroxyquinoline) aluminum film as a reference. The obtained result (≈20%) was in good agreement with the literature value.[9b]

Device Fabrication and Characterization: Glass/ITO substrates were cleaned according to standard procedures,[1a] then treated with oxygen plasma (PLASMALINE 415) for 10 min. Devices were made by thermal evaporation under a base pressure below 10^{-5} Pa. The active area of all devises is 10 mm^2. A calibrated spectrophotometer PR-650 was used to measure the electroluminescence spectrum. A Keithley 2400 source-meter unit linked to a calibrated silicon photodiode was used to measure the current-voltage-brightness characteristics. All the measurements were carried out in air at room temperature.

Data Analysis: Given the distinct emission nature of each component, the EQE of DFW-OLED1 (η_{W-1}) can be simply described as[8b,13]

$$\eta_{W-1} = \eta_{FIrpic}\chi + \eta_{Pt(ptp)_2}(1-\chi) \quad (1)$$

$$\chi = \chi_{FIrpic-emission} + \chi_{FIrpic-energytransfer} \quad (2)$$

where η_{FIrpic} is the EQE of the neat FIrpic device, $\eta_{Pt(ptp)_2}$ is the EQE of the neat $Pt(ptp)_2$ device, $\chi_{FIrpic-emission}$ and $\chi_{FIrpic-energytransfer}$ are the fractions of excitons that are directly converted into photons by FIrpic emission and energy transferred to $Pt(ptp)_2$ before the radiative decay, respectively. By fitting the DFW-OLED1 spectrum (Supporting Information Figure S5) to the electroluminescence spectra of FIrpic and $Pt(ptp)_2$, and considering photon energy in these power spectra, we calculated that the ratio of the photons emitted from FIrpic and $Pt(ptp)_2$ is approximately 1:3. Given the performance characteristics of DFW-OLED1, neat FIrpic and $Pt(ptp)_2$ devices, we calculated $\chi_{FIrpic-emission} = 46\%$ and $\chi_{FIrpic-energytransfer} = 0$ combining Equations 1 and 2 at a current density of 0.03 mA cm^{-2}, at which point DFW-OLED1, neat FIrpic and $Pt(ptp)_2$ devices all exhibit the maximum efficiency.[13] Accordingly, the fraction of excitons directly formed on $Pt(ptp)_2$ in DFW-OLED1 is $\chi_{Pt(ptp)_2-trap,W-1} = 1-\chi_{FIrpic-emission}-\chi_{FIrpic-energytransfer} = 54\%$.

In DFW-OLED2 the device EQE η_{W-2} can be described as

$$\eta_{W-2} = \eta_{FIr6}\chi' + \eta_{Pt(ptp)_2}(1-\chi') \quad (3)$$

$$\chi' = \chi_{FIr6-emission} + \chi_{FIr6-energytransfer} \quad (4)$$

where η_{FIr6} is the EQE of the neat FIr6 device, $\chi_{FIr6-emission}$ and $\chi_{FIr6-energytransfer}$ are the fractions of excitons that are directly converted into photons by FIr6 emission and energy transferred to $Pt(ptp)_2$, respectively. Following the same strategy described above, $\chi_{FIr6-emission}$ and $\chi_{FIr6-energytransfer}$ are calculated to be 49% and 33%, respectively, at a current density of 0.03 mA cm^{-2}. Therefore, the fraction of excitons directly formed on $Pt(ptp)_2$ in DFW-OLED2 is $\chi_{Pt(ptp)_2-trap,W-2} = 18\%$.

Supporting Information

Supporting Information is available from the Wiley Online Library or from the author.

Acknowledgements

This work was supported by the United States' NSF (CHE-0911690; CMMI-0963509; CHE-0840518; CHE-1004878), the Robert A. Welch Foundation (Grant B-1542), and NSF CAREER (ECCS-0950731). Dr. Q. Wang thanks the support of SRFDP (20130201120048).
Note: minor changes were made to Abstract after initial online publication to correct spelling and grammatical errors.

Received: February 20, 2014
Published online: April 16, 2014

[1] a) B. W. D'Andrade, R. J. Holmes, S. R. Forrest, *Adv. Mater.* **2004**, *16*, 624; b) S.-J. Su, E. Gonmori, H. Sasabe, J. Kido, *Adv. Mater.* **2008**, *20*, 4189; c) M. C. Gather, A. Köhnen, K. Meerholz, *Adv. Mater.* **2011**, *23*, 233; d) Q. Wang, D. G. Ma, *Chem. Soc. Rev.* **2010**, *39*, 2387.

[2] a) M. A. Baldo, C. Adachi, S. R. Forrest, *Phys. Rev. B* **2000**, *62*, 10967; b) S. Reineke, K. Walzer, K. Leo, *Phys. Rev. B* **2007**, *75*, 125328; c) N. C. Giebink, S. R. Forrest, *Phys. Rev. B* **2008**, *77*, 235215; d) D. Song, S. Zhao, H. Aziz, *Adv. Funct. Mater.* **2011**, *21*, 2311; e) S. Haneder, E. Da Como, J. Feldmann, M. M. Rothmann, P. Strohriegl, C. Lennartz, O. Molt, I. Munster, C. Schildknecht, G. Wagenblast, *Adv. Funct. Mater.* **2009**, *19*, 2416; f) H. Yersin, *Top. Curr. Chem.* **2004**, *241*, 1; g) R. C. Evans, P. Douglas, C. J. Winscom, *Coord. Chem. Rev.* **2006**, *250*, 2093.

[3] a) J. Zou, H. Wu, C.-S. Lam, C. Wang, J. Zhu, C. Zhong, S. Hu, C.-L. Ho, G.-J. Zhou, H. Wu, W. C. H. Choy, J. Peng, Y. Cao, W.-Y. Wong, *Adv. Mater.* **2011**, *23*, 2976; b) M. Cai, T. Xiao, E. Hellerich, Y. Chen, R. Shinar, J. Shinar, *Adv. Mater.* **2011**, *23*, 3590; c) B. Zhang, G. Tan, C.-S. Lam, B. Yao, C.-L. Ho, L. Liu, Z. Xie, W.-Y. Wong, J. Ding, L. Wang, *Adv. Mater.* **2012**, *24*, 1873; d) Q. Wang, J. Q. Ding, D. G. Ma, Y. X. Cheng, L. X. Wang, X. B. Jing, F. S. Wang, *Adv. Funct. Mater.* **2009**, *19*, 84; e) Y.-S. Park, J.-W. Kang, D. M. Kang, J.-W. Park, Y.-H. Kim, S.-K. Kwon, S. C. Shin, J.-J. Kim, *Adv. Mater.* **2008**, *20*, 1957; f) T.-H. Kim, H. K. Lee, O. O. Park, B. D. Chin, S.-H. Lee, J. K. Kim, *Adv. Funct. Mater.* **2006**, *06*, 611; g) B. P. Yan, C. C. C. Cheung, S. C. F. Kui, H. F. Xiang, V. A. L. Roy, S. J. Xu, C. M. Che, *Adv. Mater.* **2007**, *19*, 3599.

[4] a) S. Tao, Z. Peng, X. Zhang, P. Wang, C.-S. Lee, S.-T. Lee, *Adv. Funct. Mater.* **2005**, *15*, 1716; b) Z. Liu, Z. Bian, L. Ming, F. Ding, H. Shen, D. Nie, C. Huang, *Org. Electron.* **2008**, *9*, 171; c) Q.-X. Tong, S.-L. Lai, M.-Y. Chan, K.-H. Lai, J.-X. Tang, H.-L. Kwong, C.-S. Lee, S.-T. Lee, *Appl. Phys. Lett.* **2007**, *91*, 153504; d) S.-Y. Ku, L.-C. Chi, W.-Y. Hung, S.-W. Yang, T.-C. Tsai, K.-T. Wong, Y.-H. Chen, C.-I. Wu, *J. Mater. Chem.* **2009**, *19*, 773; e) S. Chen, Z. Zhao, B. Z. Tang, H. S. Kwok, *J. Phys. D: Appl. Phys.* **2010**, *43*, 095101; f) W. F. Xie, Z. J. Wu, S. Y. Liu, S.-T. Lee, *J. Phys. D: Appl. Phys.* **2003**, *36*, 2331.

[5] a) Y. Wang, N. Herron, V. V. Grushin, D. LeCloux, V. Petrov, *Appl. Phys. Lett.* **2001**, *79*, 449; b) S.-Y. Chang, J. Kavitha, S.-W. Li, C.-S. Hsu, Y. Chi, Y.-S. Yeh, P.-T. Chou, G.-H. Lee, A. J. Carty, Y.-T. Tao, C.-H. Chien, *Inorg. Chem.* **2006**, *45*, 137; c) Y.-H. Song, S.-J. Yeh, C.-T. Chen, Y. Chi, C.-S. Liu, J.-K. Yu, Y.-H. Hu, P.-T. Chou, S.-M. Peng, G.-H. Lee, *Adv. Funct. Mater.* **2004**, *14*, 1221; d) M. Cocchi, J. Kalinowski, L. Murphy, J. A. G. Williams, V. Fattori, *Org. Electron.* **2010**, *11*, 388; e) Z. W. Liu, M. Guan, Z. Q. Bian, D. B. Nie, Z. L. Gong, Z. B. Li, C. H. Huang, *Adv. Funct. Mater.* **2006**, *16*, 1441.

[6] a) X. H. Yang, F.-L. Wu, H. Haveriene, J. Li, C.-H. Cheng, G. E. Jabbour, *Appl. Phys. Lett.* **2011**, *98*, 033302; b) S. Liu, B. Li, L. Zhang, S. Yue, *Appl. Phys. Lett.* **2011**, *98*, 163301.

[7] a) H.-H. Chou, C.-H. Cheng, *Adv. Mater.* **2010**, *22*, 2468; b) M.-H. Tsai, Y.-H. Hong, C.-H. Chang, H.-C. Su, C.-C. Wu, A. Matoliukstyte, J. Simokaitiene, S. Grigalevicius, J. V. Grazulevicius, C.-P. Hsu, *Adv. Mater.* **2007**, *19*, 862; c) Y. T. Tao, Q. Wang, C. L. Yang, C. Zhong, J. G. Qin, D. G. Ma, *Adv. Funct. Mater.* **2010**, *20*, 2923; d) K.-Y. Lu, H.-H. Chou, C.-H. Hsieh, Y.-H. Ou Yang, H.-R. Tsai, H.-Y. Tsai, L.-C. Hsu, C.-Y. Chen, I.-C. Chen, C.-H. Cheng, *Adv. Mater.* **2011**, *23*, 4933; e) B.-S. Du, J.-L. Liao, M.-H. Huang, C.-H. Lin, H.-W. Lin, Y. Chi, H.-A. Pan, G.-L. Fan, K.-T. Wong, G.-H. Lee, P.-T. Chou, *Adv. Funct. Mater.* **2012**, *22*, 3491.

[8] a) J. Kalinowski, M. Cocchi, D. Virgili, V. Fattori, J. A. G. Williams, *Adv. Mater.* **2007**, *19*, 4000; b) Q. Wang, J. Ding, D. Ma, Y. Cheng, L. Wang, F. Wang, *Adv. Mater.* **2009**, *21*, 2397; c) J. Ye, C.-J. Zheng, X.-M. Ou, X.-H. Zhang, M.-K. Fung, C.-S. Lee, *Adv. Mater.* **2012**, *24*, 3410; d) H. Sasabe, J. Takamatsu, T. Motoyama, S. Watanabe, G. Wagenblast, N. Langer, O. Molt, E. Fuchs, C. Lennartz, J. Kido, *Adv. Mater.* **2010**, *22*, 5003; e) C. W. Seo, J. Y. Lee, *Org. Electron.* **2011**, *12*, 1459.

[9] a) C. Adachi, M. A. Baldo, M. E. Thompson, S. R. Forrest, *J. Appl. Phys.* **2001**, *90*, 5048; b) Y. Kawamura, H. Sasabe, C. Adachi, *Jpn. J. Appl. Phys.* **2004**, *43*, 7729; c) Y. Kawamura, K. Goushi, J. Brooks, J. J. Brown, H. Sasabe, C. Adachi, *Appl. Phys. Lett.* **2005**, *86*, 071104; d) W. Holzer, A. Penzkofer, T. Tsuboi, *Chem. Phys.* **2005**, *308*, 93.

[10] M. Li, W.-H. Chen, M.-T. Lin, M. A. Omary, N. D. Shepherd, *Org. Electron.* **2009**, *10*, 863.
[11] Q. Wang, I. W. H. Oswald, M. R. Perez, H. P. Jia, B. E. Gnade, M. A. Omary, *Adv. Funct. Mater.* **2013**, *23*, 5420.
[12] a) S.-H. Eom, Y. Zheng, E. Wrzesniewski, J. Lee, N. Chopra, F. So, J. G. Xue, *Org. Electron.* **2009**, *10*, 686; b) J. H. Seo, S. J. Lee, B. M. Seo, S. J. Moon, K. H. Lee, J. K. Park, S. S. Yoon, Y. K. Kim, *Org. Electron.* **2010**, *11*, 1759; c) C.-H. Hsiao, S.-W. Liu, C.-T. Chen, J.-H. Lee, *Org. Electron.* **2010**, *11*, 1500.
[13] Y. Sun, N. C. Giebink, H. Kanno, B. Ma, M. E. Thompson, S. R. Forrest, *Nature* **2006**, *440*, 908.
[14] a) M. G. Helander, Z. B. Wang, J. Qiu, M. T. Greiner, D. P. Puzzo, Z. W. Liu, Z. H. Lu, *Science* **2011**, *332*, 944; b) Y.-L. Chang, Z. B. Wang, M. G. Helander, J. Qiu, D. P. Puzzo, Z. H. Lu, *Org. Electron.* **2012**, *13*, 925.
[15] R. J. Holmes, B. W. D'Andrade, S. R. Forrest, X. Ren, J. Li, M. E. Thompson, *Appl. Phys. Lett.* **2003**, *86*, 3818.
[16] N. Matsusue, Y. Suzuki, H. Naito, *Jpn. J. Appl. Phys.* **2005**, *44*, 3691.